J. Membrane Biol. 109, 41–52 (1989)

The Journal of
Membrane Biology

Amine and Carboxylate Spin Probe Permeability in Red Cells

A. Paul Todd*, Rolf J. Mehlhorn, and Robert I. Macey
Department of Physiology-Anatomy, University of California, Berkeley, California 94720

Summary. Permeabilities for a homologous series of amine and carboxylate nitroxide spin probes were measured in human red blood cells by an electron paramagnetic resonance (EPR) method. Permeabilities determined in this study are much lower than would be predicted for a sheet of bulk hydrocarbon and the polarity of the rate-limiting region is shown to be greater than bulk hydrocarbon. This suggests that the rate-limiting region for permeation of these nonelectrolytes is somewhere in the membrane periphery rather than in the center of the membrane. The red cell membrane does not discriminate between these probes on the basis of molecular volume, as might be predicted by a simple free-volume theory of membrane permeation.

Key Words EPR spin probe · membrane permeability · nonelectrolyte · partition coefficient · red blood cell

Introduction

Biomembranes are selective permeability barriers. For molecules that do not cross the membrane through specific protein pathways, the rate of permeation must be attributed to the physical properties of both the molecule and the lipid bilayer. The existence of a lipid barrier to permeation was first inferred from the correlation of nonelectrolyte permeability in cells with solubility in nonpolar solvents (reviewed in Diamond & Wright, 1969). More recently, significant advances in understanding of membrane structure and dynamics have been achieved by the application of a variety of experimental approaches (reviewed in Fisher & Stoeckenius, 1983; Sackmann, 1983), yet the rationalization of nonelectrolyte permeability data with these findings remains an outstanding problem.

Recent workers have generally attempted to explain patterns of nonelectrolyte permeability in lipid membranes with either one of two simplified physical models of membrane structure. (*i*) Membranes behave like a thin sheet of bulk solvent such as hexadecane (Finkelstein & Cass, 1968; Finkelstein, 1976; Orbach & Finkelstein, 1980). (*ii*) Membranes resemble soft polymers such as natural rubber (Lieb & Stein, 1969, 1971, 1986). While the requisite absolute permeability measurements to test these models are accumulating for planar lipid bilayers, useful data for cells and liposomes are sparse. The purpose of this and the following paper is to examine the adequacy of these models in the light of new permeability data from red blood cells and liposomes, respectively. In the following paper we further examine whether this data can be better explained by taking into account the spatial heterogeneity of lipid membranes. Here we report permeability measurements for a homologous series of weak acid and weak base spin probes in human red blood cells by an electron paramagnetic resonance (EPR) method. Their structures are shown below:

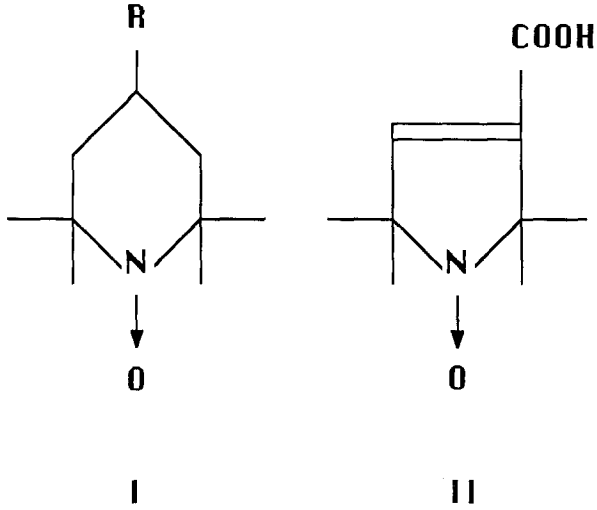

I II

We refer to the derivatives of I, 2,2,6,6-tetramethylpiperidine-1-oxyl-, as "TA", $R = NH_2$; "MTA", $R = NHCH_3$; "DMTA", $R = N(CH_3)_2$; "META", $R = NCH_3(CH_2CH_2OH)$; "CAT_1", $R = N(CH_3)_3^+$;

* *Present address:* Jules Stein Eye Institute, University of California, Los Angeles, California 90024.

and "TC", R = COOH. II is 2,2,5,5-tetramethyl-3-pyrroline-1-oxyl-3-carboxylic acid.

Titratable solutes allow investigation of a faster permeability domain than is possible with neutral solutes because their uptake kinetics may be slowed to fit within an experimentally convenient time frame by adjusting the pH (*see below*). Titratable solutes are also useful in avoiding possible unstirred layer rate limitations (Gutknecht & Tosteson, 1973).

Nitroxides are chemically stable free radicals, detectable at micromolar concentrations with an EPR spectrometer. We measure nitroxide spin probe permeabilities by employing paramagnetic quenching agents, which broaden probe signal when in the same aqueous compartment. Cells are rapidly mixed with a solution containing probe and an impermeant quencher. Probe signal is initially broadened, but increases in amplitude as it diffuses into the internal compartment where it is unquenched.

Kinetic Analysis

Amine Probe Influx Into Cells After Rapid Mixing

We assume (*i*) only the neutral form of the amine is permeant, (*ii*) the equilibrium between charged and neutral forms is very fast relative to permeation, and (*iii*) the fraction of probe in the membrane is negligible. We define permeability as the ratio of transmembrane flux per unit area to the concentration gradient between external and internal aqueous compartments. No assumption is made about the mechanism of permeation or the location of the rate-limiting step. We consider the problem of unstirred layers in a subsequent section.

Let $N \equiv$ total number of probe molecules
$s_{in}^0 \equiv$ number of neutral probe molecules inside cell/N
$s_{in}^+ \equiv$ number of charged probe moelcules inside cell/N
$s_{in} \equiv s_{in}^0 + s_{in}^+$
$s_{out}^0 \equiv$ number of neutral probe molecules outside cell/N
$s_{out}^+ \equiv$ number of charged probe molecules outside cell/N
$s_{out} \equiv s_{out}^0 + s_{out}^+$
$K_a \equiv$ amine dissociation constant
$[H^+] \equiv$ hydrogen ion concentration
$P \equiv$ measured permeability
$A \equiv$ surface area per cell
$V \equiv$ internal aqueous volume per cell
$V_{out} \equiv$ external aqueous volume per cell
$f \equiv$ internal aqueous volume/total aqueous volume.

From the definition of permeability we have

$$\frac{1}{A}\frac{ds_{in}}{dt} = P\left(\frac{s_{out}^0}{V_{out}} - \frac{s_{in}^0}{V}\right).$$

We eliminate V_{out} with the relation $V/V_{out} = f/(1-f)$, which gives us

$$\frac{ds_{in}}{dt} = \frac{PA}{V}\left(\frac{fs_{out}^0}{(1-f)} - s_{in}^0\right). \tag{1}$$

From the dissociation equilibrium for weak bases and mass conservation, one can derive the following expressions:

$$s_{out}^0 = (1 - s_{in})\beta_{out} \tag{2}$$
$$s_{in}^0 = s_{in}\beta_{in}$$

where $\beta_{out} = K_a/(K_a + [H_{out}^+])$ and $\beta_{in} = K_a/(K_a + [H_{in}^+])$. Substituting Eq. (2) into Eq. (1),

$$\frac{ds_{in}}{dt} = \frac{PA}{V}\left(\frac{f\beta_{out}}{(1-f)} - s_{in}\left[\frac{f\beta_{out}}{(1-f)} + \beta_{in}\right]\right).$$

For the initial condition, $s_{in}(0) = 0$, and assuming $[H^+]$ = constant (buffered solutions), this has the solution

$$s_{in}(t) = s_{in}(\infty)(1 - e^{-t/\tau}) \tag{3}$$

where $$s_{in}(\infty) = \frac{f\beta_{out}}{(f\beta_{out} + (1-f)\beta_{in})}$$

$$\tau = \frac{V(1-f)}{PA(f\beta_{out} + (1-f)\beta_{in})}.$$

When there is no pH gradient, $\beta_{out} = \beta_{in}$ and these expressions reduce to: $s_{in}(\infty) = f$ and $\tau = V(1-f)/(PA\beta_{out})$. For carboxylate probes, the expressions (Eq. (3)) remain the same except that $\beta_{out} = [H_{out}^+]/(K_a + [H_{out}^+])$ and $\beta_{in} = [H_{in}^+]/(K_a + [H_{in}^+])$.

If all other parameters are known, the permeability may be obtained by fitting experimental curves to Eq. (3). Solving for P and rearranging we get:

$$P = \frac{V(1-f)s_{in}(\infty)}{\tau A f \beta_{out}}. \tag{4}$$

Unstirred Layers

We now generalize to include the effect of unstirred layers on the measured permeability. Gutknecht and Walter (1981) derived the following expression for the initial flux of weak base solutes across planar

membranes, which also applies to their initial flux into vesicles:

$$\frac{1}{J_0} = \frac{1}{P_{ul}[S]} + \frac{1}{P_m[S^0]}$$

where $J_0 \equiv$ initial flux, $P_{ul} \equiv$ unstirred layer permeability, $P_m \equiv$ membrane permeability, $[S] \equiv$ initial external concentration of probe (the initial internal concentration is zero), and $[S^0] \equiv$ initial external concentration of neutral probe. In addition to the assumptions made previously that (*i*) only the neutral form is permeant and (*ii*) the equilibrium between charged and neutral forms is fast relative to permeation, this expression assumes that the unstirred layer permeabilities for the charged and neutral species are the same and that the pH is constant across the unstirred layer. Noting that $[S^0] = [S]\beta_{out}$, and $J_0 = P[S^0] = P\beta_{out}[S]$, we have:

$$\frac{1}{P\beta_{out}} = \frac{1}{P_{ul}} + \frac{1}{P_m\beta_{out}} = \frac{1}{P_{ul}} + \frac{1}{P_m} + \frac{[H^+_{out}]}{K_aP_m}. \quad (5)$$

The treatment for carboxylate solutes is similar (Gutknecht & Tosteson, 1973) except that the last term in Eq. (5) is $K_a/([H^+_{out}]P_m)$.

Experimentally, if we plot $1/P\beta_{out}$ *vs.* $[H^+_{out}]/K_a$ we obtain a slope of $1/P_m$ and an intercept of $1/P_{ul} + 1/P_m$. Thus we can measure the unstirred layer permeability by subtracting the slope from the intercept of such a plot. An alternative approach is to obtain an independent measure of P_{ul} and calculate P_m from Eq. (5) using the value of $P\beta_{out}$ at a particular $[H^+_{out}]$. P_{ul} is estimated from the apparent permeability of a rapidly permeant neutral solute.

Surface Charge

If the unstirred layer is not rate limiting, the concentration of neutral amine and carboxyl probes near the membrane surface will be identical to their bulk values, even in the presence of a surface charge. Hydrogen ion and the charged amine will be attracted to or repelled from the membrane surface to exactly the same extent. The ratio of their concentrations will remain constant and, therefore, the concentration of the neutral amine will be constant according to the amine dissociation equilibrium. Similarly, hydrogen and carboxylate ions will be attracted to or repelled from the membrane surface to exactly the opposite extent. Therefore, the product of their concentrations is constant and the concentration of the neutral carboxyl is constant according to the carboxyl dissociation equilibrium.

Materials and Methods

Preparation of Red Cells

Blood was collected from a healthy human donor in Vacutainer tubes with sodium heparin as anticoagulant. The red cells were pelleted and the serum and buffy coat removed. After resuspending in 150 mM NaCl, 3 mM $K_3Fe(CN)_6$, the red cells were again pelleted and the supernatant removed. This was repeated three times. The resulting suspension was then diluted to 20% hematocrit with more of the same solution and incubated at 5°C for at least 12 hr. Preincubation in ferricyanide, an impermeant oxidizing agent, was found to diminish a time-dependent loss of EPR signal in red cells (Ross & McConnell, 1975). Cell suspensions were kept refrigerated until immediately prior to rapid-mix experiments when they were brought to room temperature.

Quenching Solutions

For amine permeability experiments, a solution containing 90 mM (tetramethylammonium)$_2$MnEDTA and 60 mM MOPS (3-{M-Morpholino}propanesulfonic acid) or 60 mM MES (2-{N-Morpholino}ethanesulfonic acid) was titrated to the desired pH with 300 mM NaOH, then diluted to 290 mmol/kg. Osmolarity was measured with a Wescor 5500 vapor pressure osmometer. For carboxylate permeability experiments, a stock solution containing 1 M $NiSO_4$ and 1 M tetraethylenepentamine (TEPA, Strem Chemicals) was prepared and stored at 5°C. This stock solution was diluted to ~0.3 M, titrated to the desired pH with 300 mM HCl, then diluted again to 290 mmol/kg. Nickel-TEPA is a more useful quenching agent than the unchelated nickel ion because of its reduced tendency to aggregate red cells and buffer capacity.

Spin Probes and EPR Instrumentation

TEMPO (R = H), TEMPone (R = O), TEMPol (R = OH) and TA were obtained from Aldrich. II was obtained from Fisher. MTA, DMTA and META were synthesized according to Rosen (1974). TC was synthesized according to Rauckman, Rosen and Abou-Donia (1976). CAT_1 was synthesized according to Mehlhorn and Packer (1979). TEMPsulfate ($R = SO_3^-$) was synthesized according to Keith et al. (1977). EPR spectra and spectral transients were taken on a Varian E 109-E X-band EPR spectrometer interfaced to an Apple II microcomputer with an Adalab A/D converter (Interactive Microware). The minimum sampling interval was 50 msec. The spectrometer was operated at 10 mW power. All experiments were run at room temperature (15–25°C).

Spin Probe pK_a's, Solvent/Water Partition Coefficients

The amine probes were titrated against NaOH and the resulting curves (pH *vs.* amount of NaOH added) were numerically differentiated (Lanczos, 1956) to obtain the pH at the point of minimum slope, which corresponds to the pK_a.

Solvent/water partition coefficients for the neutral amine were determined from the equilibrium distribution of probe between solvent and 80 mM Na_2HPO_4, 60 mM NaOH, pH 12.0. The concentration of probe in each phase is proportional to the inte-

grated EPR signal intensity, which was obtained directly by double integration of spectra. Any incomplete separation of phases could easily be detected since probe spectra in water and hexadecane or octanol are distinguishable due to differences in linewidth, g-factor, and hyperfine splitting constant. Samples were incubated in 1.5-ml Eppendorf centrifuge tubes in a water bath at 25°C without shaking. Probe was allowed to equilibrate for at least 24 hr and successive determinations at later times were found to be constant.

As a check on our results, spin probe pK_a's and solvent/water partition coefficients were simultaneously determined from the pH-dependent partitioning between 300 mM Tris buffer (pH 8.2–10.0) and 1-octanol. Measurements of the probe concentration in aqueous and solvent phases at several pH values allowed calculation of the K_a and the neutral partition coefficient, K^0.

Let $[S_s] \equiv$ solute concentration in solvent phase
$[S_w] \equiv$ total solute concentration in aqueous phase
$[S_w^0] \equiv$ neutral solute concentration in aqueous phase.

Noting that $[S_w] = [S_w^0](K_a + [H^+])/K_a$ and defining $K^0 = [S_s]/[S_w^0]$, we obtain by substitution:

$$\frac{[S_s]}{[S_w]} = \frac{K^0 K_a}{(K_a + [H^+])}.$$

Experimentally, $[S_s]$ and $[S_w]$ are found from the integrated EPR signal intensity in nonaqueous solvent and water, respectively. Best-fit values for both K^0 and K_a were obtained by nonlinear least squares (Duggleby, 1981) and were in good agreement with the values obtained above.

Carboxylic acid pK_a's could not be determined by titration because of the low solubility of the neutral species. Instead, pK_a's were determined by the above pH-dependent partitioning method, which requires only ≃1 mM instead of ≃100 mM concentration of probe. In this case, $[S_s]/[S_w] = K^0[H^+]/(K_a + [H^+])$. The buffer used was 100 mM citrate (pH 4.2–6.0) and the solvent phase consisted of either *n*-hexadecane or 1-octanol. pK_a's obtained using the two solvents were in good agreement.

Internal Volume Measurements

Internal volumes for red cell suspensions were measured with TEMPone as described previously (Vistnes & Pushkin, 1981), (Mehlhorn, Candau & Packer, 1982). Because it is neutral, TEMPone distributes freely between aqueous compartments in a suspension of cells. If an impermeant quencher (line-broadening agent) such as $Na_2MnEDTA$ is added to the external compartment, the spectrum from this compartment is essentially removed and the amplitude of the remaining "protected" spectrum is proportional to the internal volume of the suspension, assuming linewidths are constant. TEMPone was added to an aliquot of red cells combined 1 : 1 with quencher solution to make a final concentration of 1 mM. The ratio of the amplitude for the same TEMPone concentration in an aliquot of red cells combined 1 : 1 with nonquenching buffer yielded an estimate of the fraction internal volume, *f*.

Samples for volume determinations and other equilibrium EPR measurements were loaded in 75-μl micropipettes, which were then sealed at one end with hematocrit tube sealer.

Cell Water Volumes, Surface Areas

The concentration of cells in a suspension was estimated by cyanmethemoglobin assay: 50 μl of the 20% hematocrit suspension prepared for rapid-mix experiments was added to 4 ml of cyanmethemoglobin reagent (Hycel) and allowed to stand for a few hours until hemolysis was complete. The concentration of hemoglobin was determined from the absorbance at 540 nm (hemoglobin standards were also obtained from Hycel). Assuming 29 pg Hb/cell (Osgood, 1935), we obtained directly the concentration of cells (# per cm^3). The water volume per cell (in cm^3) is given by $V = f/[\text{cells}]$. We used a standard value for the red cell surface area of 1.369×10^{-6} cm^2 (Jay, 1975).

Rapid-Mix Experiments

For spin probe permeability measurements, unbuffered red cells were rapidly mixed with an equal volume of buffered quencher solution containing 2 mM spin probe. Because probe amplitude is proportional to the number of unquenched probe molecules, the rate of emergence of the internal protected amplitude is related to the permeability of the spin probe as described in the Kinetic Analysis section. Experimentally, we followed changes in the number of internal protected probe molecules by adjusting the magnetic field to fix on a peak and scanning *vs.* time.

Rapid mixing was achieved with a custom-built stopped-flow apparatus mounted on the spectrometer. The red cell suspension and quencher solution were contained in separate syringes with plungers joined together so they could be simultaneously driven (by hand). Effluents from the syringes flowed into a simple mixing "T" immediately outside the sample cavity and thence through a glass capillary within the cavity. The distance traveled by the plungers with each experiment was controlled by adjusting a screw stop. The resonant cavity was mounted in a horizontal orientation to eliminate the effects of cell settling.

A stopped-flow experimental record for the probe TEMPol (R = OH) is shown in Fig. 1. Red cells with equilibrated internal probe from the previous experiment are pushed out of the resonant cavity by just-mixed red cells with no internal probe, leading to a steep drop in amplitude, which then recovers as probe diffuses in.

The dead time of our mixing apparatus, defined as the time it takes for sample to travel from the mixing "T" to the center of the observation port (resonant cavity), was estimated by timing the flow of a known volume of water through the apparatus and found to be ≃8 msec. The dead time was not measured for red cell suspensions, but is presumed to be somewhat longer than this because of differences in viscosity. In any case, our time resolution appears to be limited by imperfect mixing rather than dead time. The minimum of the transient in Fig. 1 corresponds to the stopping of the syringes. The initial steep, nonexponential recovery (*see below*) lasting ~400 msec must correspond to the mixing time for our apparatus. We therefore routinely ignored time points within 400 msec of the minimum deflection in our data analysis. Time constants for the equilibration of titratable probes measured in this study ranged from seconds to minutes.

A nonzero mixing time also implies a spread in "time zero" for probe uptake. Macey (1979) has shown, however, that a staggered superposition of uptake curves with identical time constants follows the same time constant at times later than the end of mixing.

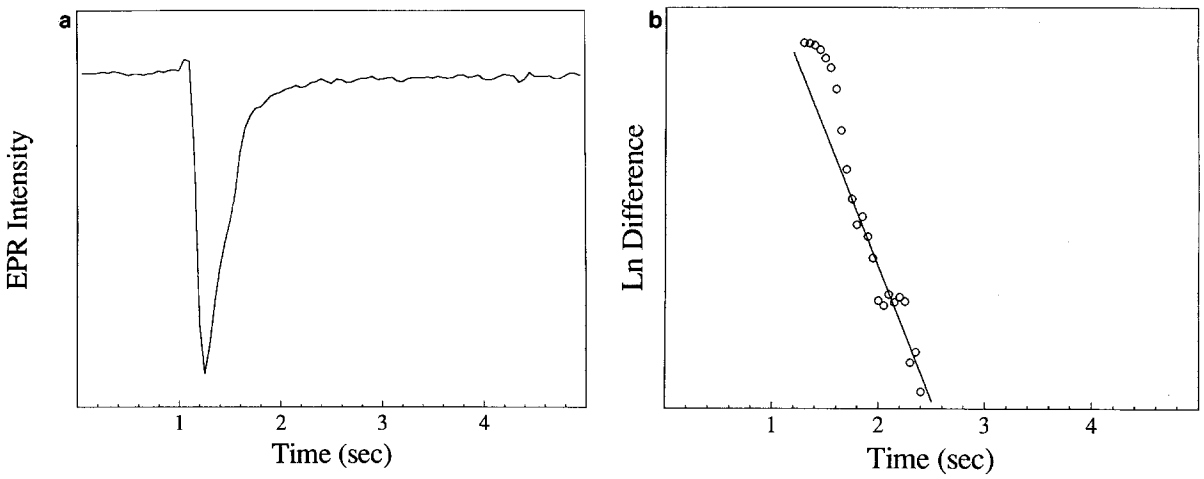

Fig. 1. (*a*) Uptake of TEMPol into RBC, pH = 7.4. TEMPol (2 mM) in MOPS/$(TMA)_2$MnEDTA buffer was rapidly mixed with unbuffered RBC (20% Hct) with 2 mM DNDS. T = 21.5°C. (*b*) Semilog plot of $\delta E(t, \delta t)$ for TEMPol uptake in Fig. 1*a*. δt = 50 msec. The first point corresponds to the minimum in Fig. 1*a*

Since unbuffered red cell suspensions were mixed with highly buffered quencher solutions, the initial external pH was set by the quencher solution, while the initial internal pH was set by the internal buffering of the red cell (pH $\simeq$ 7.2). Thus, the initial external pH could be varied without equilibrating the cells at different pH values.

Extracting permeabilities from this type of experiment requires that the transmembrane pH gradient remain constant over the time course of equilibration of probe. With our experimental design, there are newly created gradients of chloride, bicarbonate and pH across the red cell membrane upon rapid mixing, which are unstable and will tend to collapse to an equilibrium distribution primarily via the anion exchanger. The redistribution of chloride is important because it exchanges with bicarbonate on the anion exchanger and hence also leads to time-dependent pH changes. In all red cell experiments we therefore added 1 mM 4,4′-dinitro-2,2′ stilbenesulfonic acid (DNDS, ICN Pharmaceuticals), which is a reversible inhibitor of the anion exchanger. Even so, slow collapse of the pH gradient could be inferred in some experiments where the baseline drifted slowly with time. This was verified by monitoring changes in the external pH with a pH meter. In such cases, only early points on the uptake curve were used for curve fitting.

Curve-Fitting

The raw ouput in this type of experiment is a series of voltages, $E(t)$, which are linearly related to the fraction internal solute, $s_{in}(t)$. In practice, we are confronted with the problem of curve fitting the data not to Eq. (3), but to the following equation, which involves the additional parameter, $E(0)$

$$E(t) = \Delta E\,(1 - e^{-t/\tau}) + E(0)$$

where $\Delta E = E(\infty) - E(0)$. $E(0)$ does not correspond simply to the voltage at zero EPR signal because of the presence of a quenched background spectrum in the external aqueous phase. For simplicity, we reduced the number of curve-fitted parameters to two by subtracting each data point from a subsequent data point at a fixed time interval, δt.

$$\begin{aligned}\delta E(t, \delta t) &= E(t) - E(t + \delta t)\\ &= \Delta E\, e^{-t/\tau} - \Delta E\, e^{-(t+\delta t)/\tau}\\ &= \Delta E(1 - e^{-\delta t/\tau})e^{-t/\tau}.\end{aligned} \tag{6}$$

Using this procedure, we have changed the problem to that of curve fitting a new function, $\delta E(t, \delta t)$ to an exponential decay with the same time constant as before and with the amplitude, $\Delta E\ (1 - e^{-\delta t/\tau})$ from which ΔE is readily obtained. Time constants are obtained either by curve fitting $\delta E(t, \delta t)$ by nonlinear least squares (Duggleby, 1981) or from the slope of ln $\delta E(t, \delta t)$ *vs.* time. An example of such a semilog plot is shown in Fig. 1*b* for TEMPol. It can be seen that the plot deviates from a straight line for the first 400 msec, presumably due to imperfect mixing. Fitted values for the parameters are fairly insensitive to the choice of δt. We have found, however, that setting $\delta t \simeq \tau$ tends to minimize standard errors for the parameters.

Results and Discussion

Spin Probe Parameters

Spine probe pK_a's solvent/water partition coefficients, and estimated molecular volumes are given in Table 1. It may seem surprising that the carboxylate probes, TC and II partition so poorly into hexadecane, yet so favorably into octanol. The differences in partitioning into the two solvents are not nearly so great for the amine probes. The same pattern is seen in the partitioning data reported by Walter and Gutknecht (1986). For example, K_{hex} = 0.053, K_{oct} = 74 for benzoic acid while K_{hex} = 0.013 and K_{oct} = 0.66 for ethylamine.

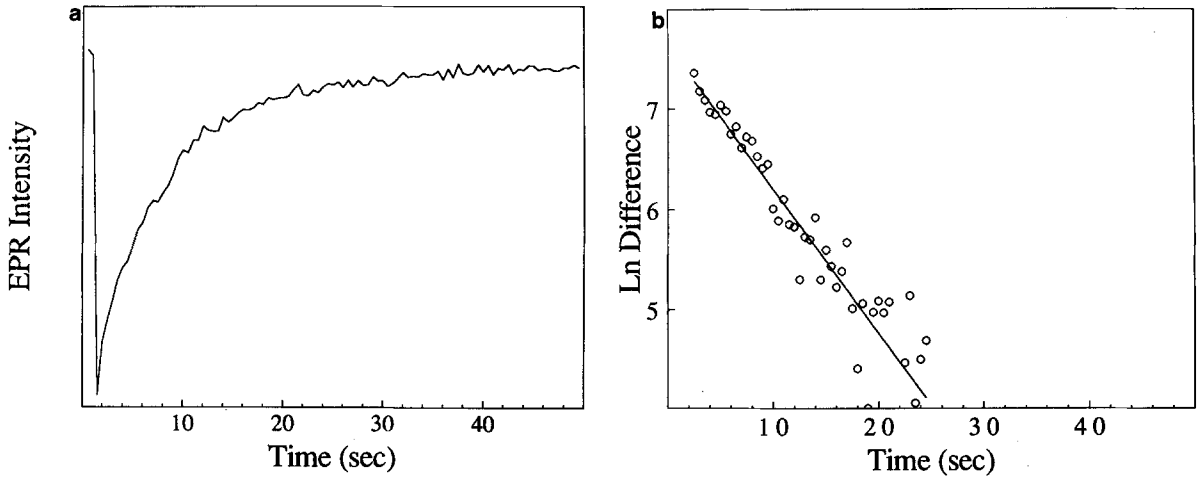

Fig. 2. (*a*) Uptake of META into RBC, pH = 6.5. META (2mM) in MOPS/$(TMA)_2$MnEDTA buffer was rapidly mixed with unbuffered RBC (20% Hct) with 2 mM DNDS. T = 21.5°C. (*b*) Semilog plot of $\delta E(t, \delta t)$ for META uptake in Fig. 2*a*

Table 1. Spin probe parameters

	pK_a	K_{hex}	K_{oct}	V
META	8.13 ± 0.02	0.0188 ± 0.0005	3.39 ± 0.17	145
TA	8.99 ± 0.01	0.0311 ± 0.0034	3.64 ± 0.07	109
MTA	9.06 ± 0.01	0.101 ± 0.002	6.88 ± 0.11	120
DMTA	8.57 ± 0.03	0.644 ± 0.017	13.6 ± 0.4	130
TC	4.12 ± 0.02	0.011 ± 0.002	22.3 ± 0.5	118
II	3.72 ± 0.02	0.015 ± 0.003	41.8 ± 1.5	105

pK_a determined from pH-dependent partitioning between 1-octanol and 300 mM Tris/HCl (pH = 8.2–10.0) or 100 mM sodium citrate (pH = 4.2–6.0). Tabulated uncertainties are standard errors for curve-fit by nonlinear least squares. By titration, pK_a(META) = 8.12 ± 0.04, pK_a(TA) = 8.94 ± 0.06.

K_{hex}, K_{oct} ≡ hexadecane/water and octanol/water partition coefficients for neutral species at 25°C. Amines were partitioned between solvent and 80 mM sodium phosphate buffer, pH = 12.0. K_{hex} is an average of four measurements while K_{oct} is an average of two measurements. Their uncertainties are standard deviations. Carboxylate determinations were from pH-dependent partitioning (*see above*).

V ≡ Van der Waals molecular volume in cm^3/mol, calculated according to Bondi (1964).

Probe Binding to Hemoglobin Is Insignificant

In calculating permeabilities, we have assumed that the amine and carboxylate probes do not bind to hemoglobin to any significant extent. This was confirmed experimentally by sonicating packed cells, centrifuging to pellet the membrane fraction, and assaying spectroscopically for probe binding to the concentrated hemoglobin in the supernatant. No significant immobilized spectral components were detected for any of the probes. We therefore conclude that probe binding to hemoglobin is negligible for purposes of our analysis.

Probe Uptake Follows Exponential Kinetics

A typical stopped-flow experimental record is shown in Fig. 2*a* for META. Cells with equilibrated internal probe from the previous experiment are pushed out of the resonant cavity by cells with no internal probe, leading to a steep drop in signal, which then recovers as probe diffuses in. A semilog plot of $\delta E(t, \delta t)$ *vs.* time for this uptake curve is shown in Fig. 2*b*. It is convincingly linear, though quite noisy at later times. The noise is accentuated in such a plot because of our use of a difference method in analyzing the data. Time constants were extracted for three such trials and averaged. Permeabilities were calculated according to Eq. (4) and are presented in Table 2. Standard errors were calculated from the propagated errors in all measured quantities according to Young (1962).

Only Neutral Species Permeate

In our analysis, we assume that the charge probe is impermeant on the time scale of our experiments. We justify this assumption by the fact that CAT_1, a permanently charged quaternary amine nitroxide, does not enter the red cell to a detectable extent over a period of several hours. TEMPsulfate, a monovalent anion ($R = SO_3^-$), does not enter to a detectable extent within 15 min.

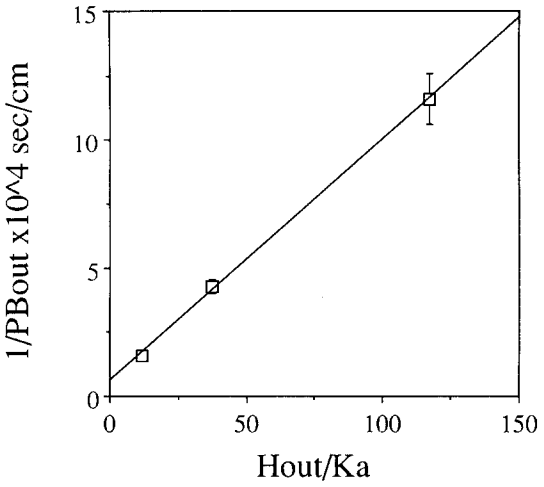

Fig. 3. pH dependence of DMTA permeability in RBC. Slope = $1/P_m = (0.944 \pm 0.026) \times 10^3$ sec/cm. Intercept = $1/P_{ul} + 1/P_m = (5.93 \pm 1.82) \times 10^3$ sec/cm

Unstirred Layer Permeability

To ascertain that our measured permeabilities correspond to the membrane and not the unstirred layer, we investigated the pH-dependence of DMTA permeability. In Fig. 3, we have plotted $1/P\beta_{out}$ *vs.* H_{out}/K_a as described in the Kinetic Analysis section. The reciprocal of the slope was found to be $(1.06 \pm 0.03) \times 10^{-3}$ cm/sec, which corresponds to the membrane permeability. By subtracting the slope from the intercept and taking the reciprocal, we obtain the unstirred layer permeability for this system, which was $(2.00 \pm 0.73) \times 10^{-4}$ cm/sec.

We also measured the apparent permeability of the neutral spin probe, TEMPol (Fig. 1*a*), which is believed to be fast enough to be entirely unstirred layer limited. P_{ul} obtained in this manner was $(1.86 \pm 0.36) \times 10^{-4}$ cm/sec, in excellent agreement with the result for DMTA. Corrections for unstirred layers, according to Eq. (5) in the Kinetic Analysis section, are negligible for DMTA at pH 6.5 and lower and negligible for the other probes at all pH values at which experiments were carried out.

Amine and Carboxylate Probes Follow Lipid Pathway

The red cell amine and carboxylate permeabilities are given in Table 2. The carboxylate measurements required some additional controls.

There are two protein pathways for anions in red cells, which could potentially short-circuit diffusion of the neutral species through the lipid pathway: the anion exchanger and the monocarboxylate transporter (Deuticke, Rickert & Beyer, 1978). It was found that the initial rates of uptake of both carboxylate probes at pH 5 were decreased in the absence of the inhibitor DNDS (Fig. 4). Under these conditions, rapid collapse of the pH gradient via the anion exchanger will raise the external pH and slow initial uptake of the neutral form, whereas any movement of probe through the exchanger will accelerate initial uptake. Because a slowing of uptake was observed, it is apparent that pH equilibrates more quickly through the exchanger than do the carboxylate probes. Since pH equilibration was satisfactorily inhibited by 1 mM DNDS, movement of probe through the exchanger cannot have affected carboxylate permeability measurements under these conditions.

We also investigated the possibility that TC and II permeate via the monocarboxylate transporter, which is completely inhibited by 3 μmol/(ml cells) *p*-chloromercuriphenyl-sulfonic acid (PCMBS, Sigma), (Deuticke et al., 1978) with lactate as substrate. Solid PCMBS was dissolved in cell suspensions to obtain this concentration immediately prior to control experiments. Time constants with and without the inhibitor, PCMBS, differed by only 12% for both probes, which could well be due to nonspecific effects of PCMBS on the red cell membrane.

Table 2. Amine and carboxylate spin probe permeabilities in red cells (21°C)

	$P \times 10^4$	P/P_{calc}
pH = 6		
META	0.774 ± 0.078	0.0021
TA	1.10 ± 0.12	0.0018
MTA	2.46 ± 0.26	0.0012
DMTA	10.2 ± 1.2	0.00079
pH = 5		
TC	1.89 ± 0.13	0.0086
II	3.57 ± 0.23	0.012

$P_{calc} \equiv KD/\Delta x$; $K \equiv K_{hexadecane}$; $D = 10^{-6}$ cm²/sec; $\Delta x = 50$ *A*.

Red Cell Permeability and Solubility in Nonpolar Solvents

It has been widely assumed that the rate-limiting step in solute permeation of biomembranes is diffusion through the bilayer interior, rather than adsorption/desorption at the aqueous/membrane interface. In the second paper in this series (Todd, Mehlhorn & Macey, 1989), we demonstrate that TA and MTA are indeed not rate limited by adsorption/desorption at the interface in PC/PA liposomes, nor is TA in PC/CH/PA liposomes. Such a demonstra-

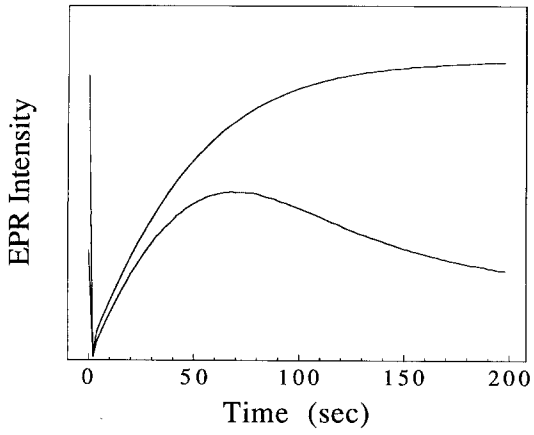

Fig. 4. DNDS slows collapse of pH gradients during uptake of II into RBC. II (2 mM) in Nickel/TEPA buffer (pH = 5.5) was rapidly mixed with unbuffered RBC (20% Hct) ± 2 mM DNDS. T = 21.5°C. Upper curve: with DNDS. Lower curve: without DNDS. Internal II first increases after rapid mixing, then decreases as pH gradient moves towards new equilibrium

tion was not possible with our probes in red cells because it requires significant binding of probe to the membrane. We will assume provisionally that some diffusion step within the bilayer is also rate limiting for all the probes in this study with red cells.

Many investigators have attempted to account for solute permeabilities in plant and animal cells by a homogeneous solubility-diffusion mechanism whereby

$$P = KD/\Delta x$$

with $K \equiv$ membrane/water partition coeeficient, $D \equiv$ intramembrane diffusion coefficient and $\Delta x \equiv$ membrane thickness. It has generally been found that $P \propto K_s$ where K_s is the solvent/water partition coefficient for an appropriate solvent thought to resemble the bilayer interior such as olive oil. Such findings are consistent with a homogeneous solubility-diffusion barrier. If this model is correct, we should be able to predict measured permeabilities from estimates of K, D, and Δx. Finkelstein (1976) reasoned that since the lipid tails are composed of hydrocarbon, the membrane interior should resemble a bulk hydrocarbon with respect to both partitioning and diffusion of solutes. ^{14}C tracer permeabilities were measured for a series of ten nonelectrolytes in egg PC planar lipid bilayers and reasonably good quantitative agreement was obtained with the calculated permeabilities for a 50-A thick sheet of hexadecane (Finkelstein & Cass, 1968; Finkelstein, 1976; Orbach & Finkelstein, 1980). Diffusion coefficients in hexadecane were assumed to be similar to measured values in water ($\sim 10^{-5}$ cm^2/sec). These solutes covered a range in permeability of nearly five orders of magnitude and, with one exception, were within a factor of 5 or better of the predicted value. A log/log plot of permeability *vs.* the product of the hexadecane/water partition coefficient, K_{hex}, and the aqueous diffusion coefficient, had the predicted slope of one (Orbach & Finkelstein, 1980). Similar results may be obtained from data compiled by Walter and Gutknecht (1986) and are presented in the following paper (Todd et al., 1989).

Table 3. *n*-Alkanol permeabilities in human red cells (Brahm, 1983)

	$P \times 10^3$	P/P_{calc}
Methanol	3.7	0.011
Ethanol	2.1	0.0024
Propanol	6.5	0.0018
Butanol	61.0	0.0048
Hexanol	8.7	0.00007

$P_{calc} \equiv KD/\Delta x$; $K \equiv$ olive oil/water partition coefficient; $D \equiv$ diffusion coefficient in H_2O; $\Delta x = 50$ *A*;

Permeabilities were also measured for some of the same solutes in egg PC/cholesterol (PC/CL) and sphingomyelin/cholesterol (SM/CL) planar lipid bilayers (Finkelstein, 1976). The calculated permeabilities for a hexadecane sheet were too high on average by more than an order of magnitude for PC/CL bilayers and by more than two orders of magnitude for SM/CL bilayers. Evidently a bulk hydrocarbon sheet is a less satsifactory model for these membranes.

We have made a similar comparison between the predictions for a hydrocarbon sheet and measured red cell permeabilities for the amine and carboxylate spin probes. The diffusion coefficient in hexadecane is not known for these probes, so we have made the conservative assumption that $D \simeq 10^{-6}$ cm^2/sec. It can be seen in Table 2 that red cell permeabilities are two or more orders of magnitude lower than the permeabilities calculated for a sheet of hexadecane 50 Å thick. Evidently, K, D, or both are lower than in bulk hydrocarbon. A similar discrepancy is found for the *n*-alkanol red cell permeabilities reported by Brahm (1983) as seen in Table 3. Thus, red cell membranes resemble planar lipid bilayers containing cholesterol and sphingomyelin in their relative impermeability to nonelectrolytes. This is consistent with their lipid composition of 25% cholesterol, 18% sphingomyelin and only 23% PC (Korn, 1966).

Cholesterol (McConnell & McFarland, 1972) and cholesterol with sphingomyelin (Todd et al.,

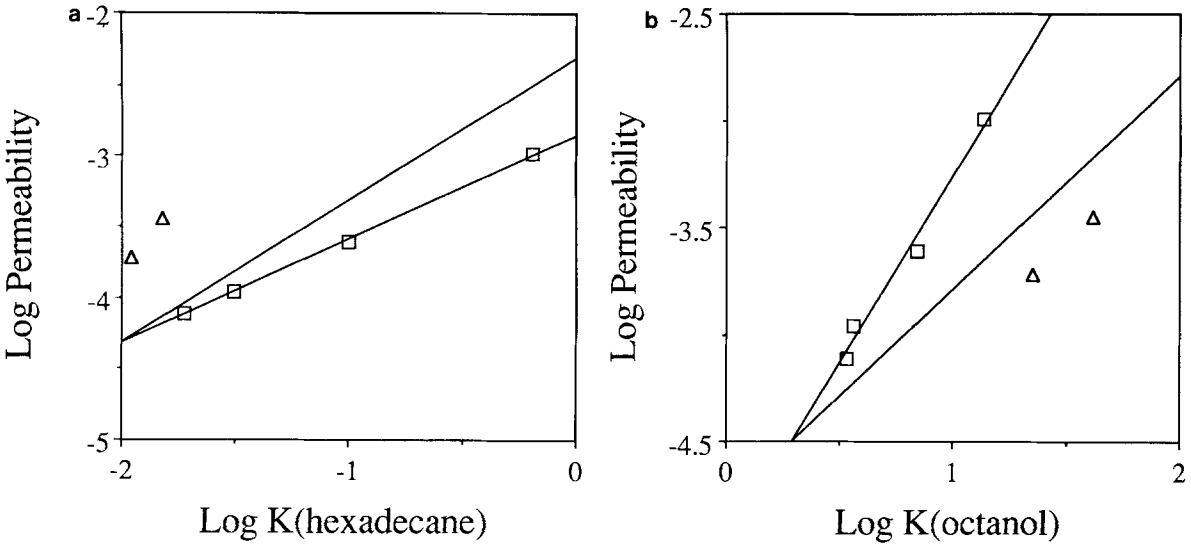

Fig. 5. (*a*) RBC spin probe permeability (21°C) *vs.* *n*-hexadecane/water partition coefficient (25°C). Squares: amine probes. Triangles: carboxylate probes. Error bars are within the size of the symbols. Lower line is best-fit slope through amine points (0.73 ± 0.02). Upper line has unity slope. (*b*) RBC spin probe permeability (21°C) *vs.* 1-octanol/water partition coefficient (25°C). Upper line is best-fit slope through amine points (1.76 ± 0.16). Lower line has unity slope

1989) have been shown to increase order in lipid membranes, which may explain their effect on nonelectrolyte permeability. Spin-labeled stearic acids and spin-labeled cholestane do exhibit greater motional restriction in oriented red cell membranes than in sonicated phospholipid dispersions (Hubbell & McConnell, 1969). Spin-labeled stearic acids also indicate a high degree of order in unoriented red cell ghost membranes (Todd et al., 1989). A high degree of membrane order suggests that the partitioning of solutes will be unfavorable and the diffusion of solutes slow. It has previously been shown that the hydrophobic spin probe, TEMPO, partitions relatively poorly into red cells (Hubbell & McConnell, 1968).

We have also plotted red cell permeability *vs.* solvent partitioning. For the amines, the plot of permeability *vs.* K_{hex} has a slope less than 1 while the plot *vs.* K_{oct} has a slope greater than 1 (Fig. 5*a*,*b*). Taken at face value, this result implies that the polarity of the rate-limiting region of the membrane is intermediate between hexadecane and octanol. This suggests that the rate-limiting region for these probes is not in the center of the bilayer, which is expected to have the same polarity as bulk hydrocarbon (Flewelling & Hubbell, 1986).

No Apparent Volume Dependence

There have been persistent reports that the size selectivity of biomembranes to nonelectrolytes is steeper than simple diffusion through water. This was found for *Nitella* cells (Collander, 1954, 1960), *Chara* cells (Lieb & Stein, 1969), multilamellar liposomes (Cohen & Bangham, 1972; Cohen, 1975) and planar lipid bilayers (Wolosin & Ginsburg, 1975; Wolosin et al., 1978). To explain such observations, Lieb and Stein (1969) suggested that membranes behave like soft polymers such as natural rubber with respect to the diffusion of solutes. Diffusion in such media depends on the formation of a succession of holes of sufficient size to accommodate the solute. Since large holes are less favored energetically than small holes and small holes exclude larger solutes, soft polymers select against larger solutes.

In Fig. 6*a* and *b* we have normalized red cell permeabilities for hydrophobicity (by K_{hex} and K_{oct}, respectively) and plotted them against molecular volume. While red cell permeability data taken from Lieb and Stein (1986) do show a steep negative volume dependence, our amine and carboxylate spin probe data do not. Assuming both data sets are representative, this suggests a break in volume dependence at 50–100 ml/mol.

Lieb and Stein recently (1986) refined the soft polymer model and applied it to already extant nonelectrolyte permeability data in human red cells. They found that a plot of P *vs.* K_{hex} was a poor fit to a straight line with unity slope. A much better fit could be obtained if the permeabilities were first "corrected" for their Van der Waals volumes by

$$P^{v=0} = P \exp(-2.3 m_v V)$$

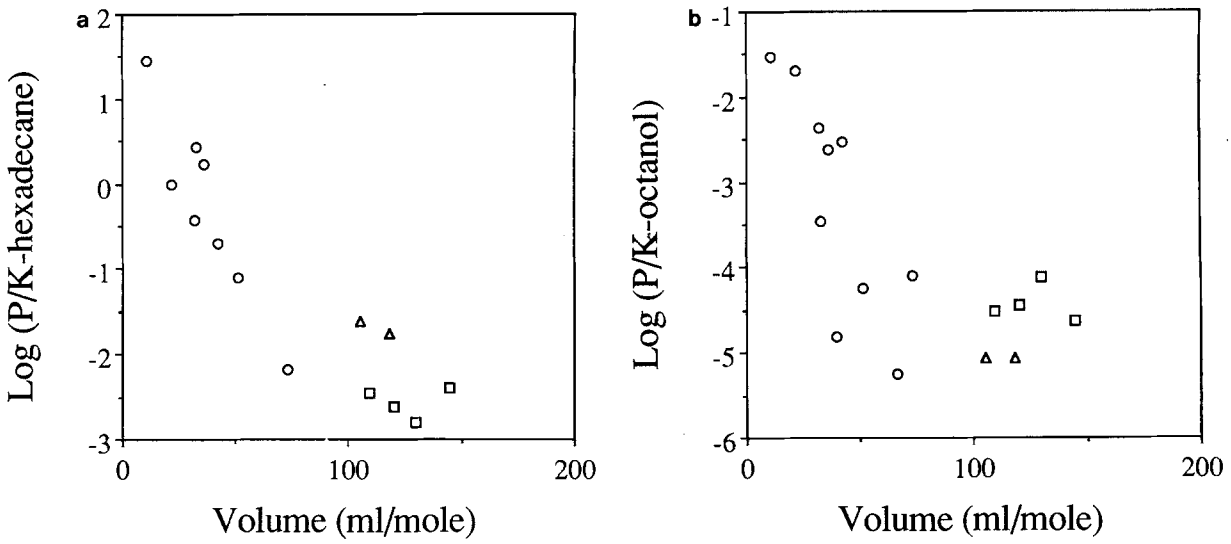

Fig. 6 (*a*) RBC spin probe permeability, corrected by hexadecane/water partitioning, *vs.* Van der Waals molecular volume. Squares: amine probes. Triangles: carboxylate probes. Error bars are within the size of the symbols. Circles: data from Lieb and Stein (1986). (*b*) RBC spin probe permeability, corrected by octanol/water partitioning, *vs.* Van der Waals molecular volume

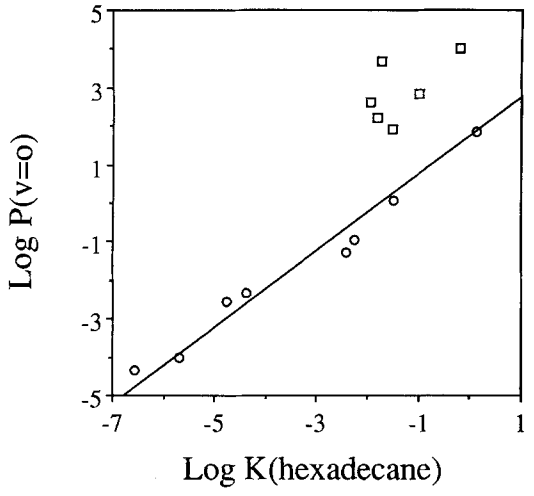

Fig. 7. "Size-corrected" permeability *vs.* hexadecane/water partition coefficient. Circles: data from Lieb and Stein (1986). Squares: data for amine and carboxylate spin probes in this study

where $P \equiv$ measured permeability coefficient, $P^{v=0} \equiv$ the zero volume or volume corrected permeability, $V \equiv$ Van der Waals volume (cm^3/mol) and m_v is a fitted parameter, the slope of a plot of log (P/K_{hex}) *vs.* V. The same procedure was employed using other model solvents, but the final fit was best using hexadecane, from which Lieb and Stein inferred that hexadecane best mimics the solubility characteristics of the rate-limiting region of the red cell membrane interior.

The fact that size selectivity for these solutes in red cells depends exponentially on solute molecular volume coincides with the theoretical probability of occurrence of holes of volume greater than or equal to the solute volume in a polymer (Cohen & Turnbull, 1959). This probability should be proportional to the diffusion coefficient. It is therefore argued that the red cell membrane resembles a soft polymer such as natural rubber with respect to the permeation of nonelectrolytes.

We have combined Lieb and Stein's plot of $P^{v=0}$ *vs.* K_{hex} for eight solutes with our own results (Fig. 7). As can be seen, their data fits a straight line with unity slope, whereas ours fails to follow the same overall trend.

It is interesting to consider why some workers have observed a negative volume dependence, while others have not (Orbach & Finkelstein, 1980). It has been suggested (Wolosin et al., 1978) that Finkelstein used solutes of similar minimum cross-sectional area and that this, and not molecular volume, is the critical parameter. Since our probes are variations on the same nitroxide theme, they should also have very similar minimum cross-sectional areas. Gutknecht and Walter (1986) observed a clear negative volume dependence in planar membranes for solutes smaller than 50 Da while larger solutes showed only a weak volume dependence. These authors point out that a steeper dependence for small solutes is characteristic of the behavior of soft polymers. This behavior is not predicted by free-volume theory, however (Cohen & Turnbull, 1959; Blank, 1962, 1964). Since the molecular weights of our sol-

utes all greatly exceed 50 Da, their lack of volume dependence may be inconsistent with a "naive" free-volume theory, but consistent with the behavior of real soft polymers. It may be that the Lieb and Stein theory applies only to small solutes, which can move through preformed holes or kinks in biomembranes (Trauble, 1971). For larger solutes (>50 Da), diffusion through the bilayer must involve the cooperative interaction of several lipid molecules with the solute, which apparently makes the process much less dependent on solute molecular volume.

This work was supported by NIH Grant Nos. GM-18819, HL-37593 (to RIM) and AG 04818 (to RJM).

References

Blank, M. 1962. Monolayer permeability and the properties of natural membranes. *J. Phys. Chem.* **66:**1911–1918

Blank, M. 1964. An approach to a theory of monolayer permeation by gases. *J. Phys. Chem.* **68:**2793–2800

Bondi, A. 1964. Van der Waals volumes and radii. *J. Phys. Chem.* **68:**441–451

Brahm, J. 1983. Permeability of human red cells to a homologous series of aliphatic alcohols: Limitations of the continuous flow-tube method. *J. Gen. Physiol.* **81:**283–304

Cohen, B.E. 1975. The permeability of liposomes to nonelectrolytes. II: The effect of nystatin and gramicidin A. *J. Membrane Biol.* **20:**235–268

Cohen, B.E., Bangham, A.D. 1972. Diffusion of small non-electrolytes across liposome membranes. *Nature (London)* **236:**173–174

Cohen, M.H., Turnbull, D. 1959. Molecular transport in liquids and gases. *J. Chem. Phys.* **31:**1164–1169

Collander, R. 1954. The permeability of *Nitella* cells to nonelectrolytes. *Physiol. Plant.* **7:**420–445

Collander, R. 1960. The permeation of polypropylene glycols. *Physiol. Plant.* **13:**179–185

Deuticke, B., Rickert, I., Beyer, E. 1978. Stereoselective, SH-dependent transfer of lactate in mammalian erythrocytes. *Biochim. Biophys. Acta* **507:**137–155

Diamond, J.M., Wright, E.M. 1969. Biological membranes: The physical basis of ion and nonelectrolyte selectivity. *Annu. Rev. Physiol.* **31:**581–646

Duggleby, R.G. 1981. A nonlinear regression program for small computers. *Anal. Biochem.* **110:**9–18

Finkelstein, A. 1976. Water and nonelectrolyte permeability of lipid bilayer membranes. *J. Gen. Physiol.* **68:**127–135

Finkelstein, A., Cass, A. 1968. Permeability and electrical properties of thin lipid membranes. *J. Gen. Physiol.* **53:**145s–172s

Fisher, K.A., Stoeckenius, W. 1983. Biomembrane models. *In:* Biophysics. W. Hoppe et al., editors. pp. 413–425. Springer-Verlag, Berlin

Flewelling, R.F., Hubbell, W.L. 1986. The membrane dipole potential in a total membrane potential model. *Biophys. J.* **49:**541–552

Gutknecht, J., Tosteson, D.C. 1973. Diffusion of weak acids across lipid bilayer membranes: Effects of chemical reactions in the unstirred layers. *Science* **182:**1258–1261

Gutknecht, J., Walter, A. 1981. Histamine, theophylline and tryptamine transport through lipid bilayer membranes. *Biochim. Biophys. Acta* **649:**149–154

Hubbell, W.L., McConnell, H.M. 1968. Spin-label studies of the excitable membranes of nerve and muscle. *Proc. Natl. Acad. Sci. USA* **61:**12–16

Hubbell, W.L., McConnell, H.M. 1969. Orientation and motion of amphiphilic spin labels in membranes. *Proc. Natl. Acad. Sci. USA* **64:**20–27

Jay, A.W.L. 1975. The geometry of the human erythrocyte. *Biophys. J.* **15:**205–222

Keith, A.D., Snipes, W., Mehlhorn, R.J., Gunter, T. 1977. Factors restricting diffusion of water-soluble spin labels. *Biophys. J.* **19:**205–218

Korn, E.D. 1966. The structure of biological membranes. *Science* **153:**1491–1498

Lanczos, C. 1956. Applied Analysis. Prentice Hall, Englewood Cliffs (NJ)

Lieb, W.R., Stein, W.D. 1969. Biological membranes behave as non-porous polymeric sheets with respect to the diffusion of non-electrolytes. *Nature (London)* **224:**240–243

Lieb, W.R., Stein, W.D. 1971. The molecular basis of simple diffusion within biological membranes. *In:* Current Topics in Membranes and Transport. F. Bronner and A. Kleinzeller, editors. pp. 1–39. Academic, New York

Lieb, W.R., Stein, W.D. 1986. Non-stokesian nature of transverse diffusion within human red cell membranes. *J. Membrane Biol.* **92:**111–119

Macey, R.I. 1979. Transport of water and nonelectrolytes across red cell membranes. *In:* Membrane Transport in Biology II. G. Giebisch, D.C. Tosteson, and H.H. Ussing, editors. pp. 1–57. Springer-Verlag, Berlin

McConnell, H.M., McFarland, B.G. 1972. The flexibility gradient in biological membranes. *Ann. NY Acad. Sci.* **195:**207–217

Mehlhorn, R.J., Candau, P., Packer, L. 1982. Measurement of volumes and electrochemical gradients with spin probes in membrane vesicles. *Methods Enzymol.* **88:**715–762

Mehlhorn, R.J., Packer, L. 1979. Membrane surface potential measurements with amphiphilic spin labels. *Methods Enzymol.* **56:**515–526

Orbach, E., Finkelstein, A. 1980. The nonelectrolyte permeability of planar lipid bilayer membranes. *J. Gen. Physiol.* **75:**427–436

Osgood, E.E. 1935. Normal hematologic standards. *Arch. Intern. Med.* **56:**849–863

Rauckmann, E.J., Rosen, G.M., Abou-Donia, M.B. 1976. Synthesis of a useful spin labeled probe. *J. Org. Chem.* **41:**564–565

Rosen, G.M. 1974. Use of sodium cyanoborohydride in the preparation of biologically active nitroxides. *J. Med. Chem.* **17:**358–360

Ross, A.H., McConnell, H.M. 1975. Permation of a spin-label phosphate into the human erythrocyte. *Biochemistry* **14:**2793–2798

Sackmann, E. 1983. Physical foundations of the molecular organization and dynamics of membranes. *In:* Biophysics. W. Hoppe et al., editors. pp. 425–457. Springer-Verlag, Berlin

Todd, A.P., Mehlhorn, R.J., Macey, R.I. 1989. Amine spin probe permeability in sonicated liposomes. *J. Membrane Biol.* **109:**53–64

Trauble, H. 1971. The movement of molecules across lipid membranes: A molecular theory. *J. Membrane Biol.* **4:**193–208

Vistnes, A.I., Pushkin, J.S. 1981. A spin label method for measuring internal volumes in liposomes or cells, applied to Ca-

dependent fusion of negatively charged vesicles. *Biochim. Biophys. Acta* **644:**244–250

Walter, A., Gutknecht, J. 1986. Permeability of small nonelectrolytes through lipid bilayer membranes. *J. Membrane Biol.* **90:**207–217

Wolosin, J.M., Ginsburg, H. 1975. The permeation of organic acids through lecithin bilayers: Resemblance to diffusion in polymers. *Biochim. Biophys. Acta* **389:**20–33

Wolosin, J.M., Ginsburg, H., Lieb, W.R., Stein, W.D. 1978. Diffusion within egg lecithin bilayers resembles that within soft polymers. *J. Gen. Physiol.* **71:**93–100

Young, H.D. 1962. Statistical Treatment of Experimental Data. McGraw-Hill, New York

Received 19 September 1988; revised 3 January 1989